Self-trapped exciton recombination in silicon nanocrystals

A. Yu. Kobitski* and K. S. Zhuravlev
Institute of Semiconductor Physics, 630090 Novosibirsk, Russia

H. P. Wagner and D. R. T. Zahn
Institut für Physik, TU Chemnitz, D-09107, Chemnitz, Germany

(Received 30 June 2000; revised manuscript received 6 November 2000; published 2 March 2001)

In this paper we investigate the time-resolved and stationary photoluminescence (PL) of silicon nanocrystals fabricated in a silicon oxide matrix. The PL intensity reveals a nonexponential decay for all temperatures which can be fitted by a ''stretch''-exponential function. From 60 down to 5 K an increase of decay time is observed going along with a decrease of the PL intensity. In addition the PL spectra show a shape change during the decay. The experimental data are interpreted in the model of self-trapped excitons (STE) which are localized in a Si-Si dimer. A numerical simulation of this model provides the radiative and nonradiative recombination times of the STE transition, the energy of the STE singlet-triplet splitting and the height of the self-trapped barrier.

DOI: 10.1103/PhysRevB.63.115423 PACS number(s): 61.46.+w, 78.20.−e, 78.47.+p, 71.35.Aa

I. INTRODUCTION

After the observation of efficient luminescence from porous silicon in the visible spectral range at room temperature by Canham[1] wide investigations have been devoted to study silicon-based nanostructures for possible applications as light emitting devices. Silicon nanocrystals which are fabricated by silicon ion implantation into silicon oxide with subsequent thermal annealing are promising candidates for light emitters. Recently, the visible and near-infrared photoluminescence (PL) of silicon nanocrystals in the 1.5–1.7 eV range was attributed to the recombination via surface states on silicon nanocrystals.[2–4] Using empirical tight-binding and first-principle local-density calculations Allan *et al.*[5] demonstrated that these states can exist as ''self-trapped excitons'' (STE) in Si-Si dimers which are located on the surface of Si nanocrystals. However, a clear experimental confirmation of this model was not yet presented.

In our paper we present spectrally and time resolved PL measurements which were performed in the 5 to 300 K temperature range. A combined analysis of the decay time dependence on the emission energy and temperature specifies and validates the model of the STE recombination in silicon nanostructures.

II. EXPERIMENTAL DETAILS

The investigated samples were prepared from 500 nm thick layers of SiO_2 grown on Si which were implanted first with 200 and subsequently with 100 keV Si^+ at a dose of 1×10^{17} cm^{-2}. Subsequently, they were annealed for 1 s at 1200 °C and for 30 min at 400 °C. Transmission electron microscopy and Raman scattering investigations proved the formation of crystalline silicon clusters with an average size of 3.5 nm. A more detailed description of the sample preparation and characterization is given elsewhere.[6] A continuous wave (cw) Ar-ion laser operating at $\lambda=488$ nm with a maximum power density of 1 $kW\cdot cm^{-2}$ was used to study the steady-state PL. The time-resolved PL was investigated using a pulsed N_2 laser ($\lambda=337$ nm) with a pulse duration of 7 ns and a peak power density of 4 $kW\cdot cm^{-2}$. The PL signal was spectrally resolved and detected by the combination of a double diffraction grating monochromator equipped with a cooled S-1 photomultiplier operating in the photon counting mode. The PL spectra were corrected for the wavelength dependent sensitivity of the system, which was determined by black-body-radiation measurements.

III. EXPERIMENTAL RESULTS

In Fig. 1 a typical room-temperature steady-state PL spectrum of Si nanocrystals and a set of time-resolved PL spectra measured at 300 K as a function of the delay time after the excitation pulse are shown. The steady-state spectrum comprises an asymmetrical band around 1.5 eV with a width of

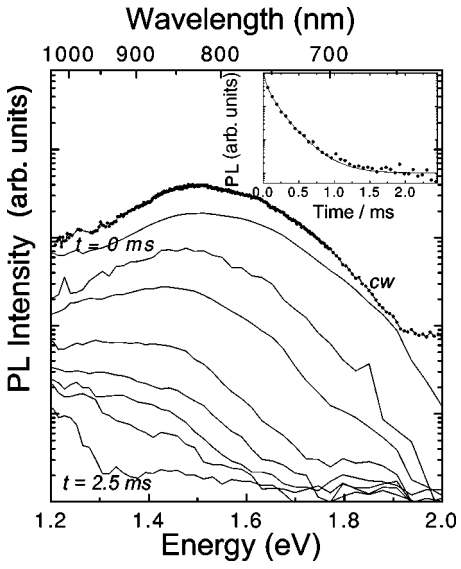

FIG. 1. Room temperature steady-state PL spectrum of Si nanocrystals and evolution of the transient PL spectrum with time. The inset shows the decay curve integrated over the band spectrum.

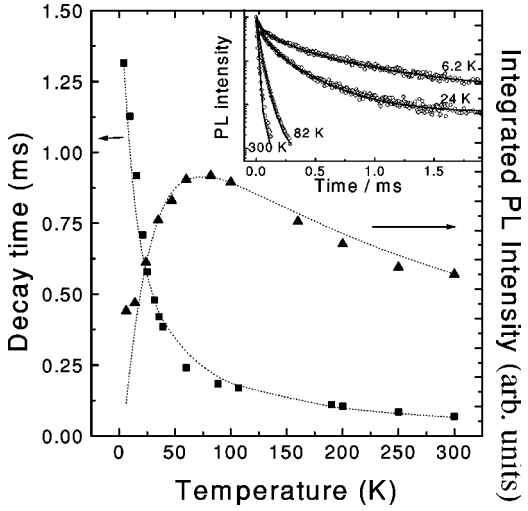

FIG. 2. Experimental (symbols) and calculated (dots) temperature dependence of the decay time (squares) and integrated PL intensity (triangles) of the investigated Si nanocrystals.

about 300 meV. Previously,[4] we noted that no shape changes were observed in time-resolved PL spectra monitored on a microsecond decay scale. However, as shown in Fig. 1 a ''red''-shift of the peak position is clearly observable in the millisecond decay range. The inset to Fig. 1 shows the decay curve of the integrated PL spectrum. The decay is nonexponential, and can be fitted by a ''stretch-exponential'' function

$$I(t) = I_0 \cdot \exp\{-(t/\tau)^{\beta}\} \tag{1}$$

where τ is the decay time and β is the dispersion factor. The approximation of the decay curve at room temperature gives a value of $\tau = 60$ μs and $\beta = 0.73$ for the decay time and the dispersion factor, respectively.

Inset to Fig. 2 shows PL decay curves taken at 6.2, 24, 82, and 300 K and their fitting by Eq. (1). This approximation gives values of about 1315, 600, 175, and 60 μs for the decay time and 0.5, 0.57, 0.73, and 0.73 for the dispersion parameter β, correspondingly. In Fig. 2 the temperature dependence of the decay time derived from Eq. (1) and of the integral PL intensity are shown. From 60 down to 4 K the decay time clearly increases which is accompanied by a reduction of the PL intensity. At about 60 K the PL intensity reveals a maximum value and then at higher temperatures begins to decrease with a moderate temperature dependence. The corresponding values of the temperature dependent dispersion factors $\beta(T)$ are given in Fig. 3 showing a constant parameter value $\beta = 0.73$ above 60 K and a clear decrease of $\beta(T)$ below 60 K.

Figure 4 demonstrates the spectral dependence of the decay time in the range between 1.4 to 1.8 eV at different temperatures. Hereby we used the $\beta(T)$ values obtained from the integrated PL decay where we approximately assumed a constant dispersion parameter within the investigated spectral range showing a good agreement between experimentally observed and calculated decay curves. At room

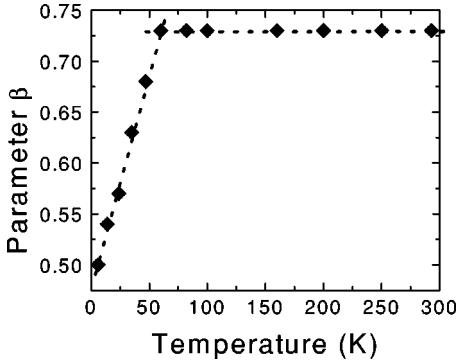

FIG. 3. Temperature dependence of the dispersion factor $\beta(T)$. The dotted line plotted as a guide for the eye.

temperature the decay time exponentially decreases with increasing energy giving a parameter γ of about 0.3 eV according to the relation $\tau \sim \exp(-E/\gamma)$, which is explained later, while the decay times show a more complicated spectral dependence at lower temperatures.

IV. DISCUSSION

A. Radiative and nonradiative mechanisms of recombination

The results obtained are explained in the model of a STE recombination on the boundary between silicon nanocrystals and the silicon dioxide as suggested by Allan *et al.*[5] In addition, nonradiative recombination was taken into account. It was shown that the luminescence efficiency in silicon nanocrystals fabricated by chemical vapor deposition is less than 1% at room temperature.[7] The estimate of the luminescence efficiency of our samples gives a similar value. Furthermore, the integrated PL shown in Fig. 2 increases not more than 1.5 times with decreasing temperature Therefore we conclude that nonradiative recombination is dominating in the whole temperature range.

As schematically sketched in Fig. 5 excitons can recombine radiatively or nonradiatively from the delocalized excited electronic state (E) or from a self-trapped exciton state (STE) to the ground state (G). Since radiative transitions

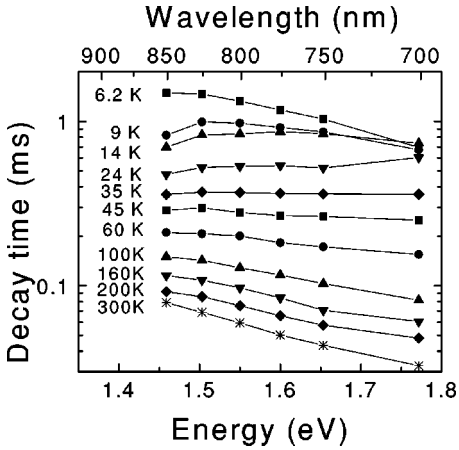

FIG. 4. Spectral dependence of the decay time at different temperatures.

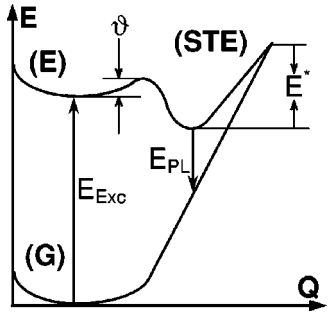

FIG. 5. Schematical configuration diagram of a Si-Si dimer at the nanocrystal-amorphous matrix boundary. It shows an excitation from the ground state (G) into the first excited electronic state (E) and radiative emission from the self-trapped exciton state (STE) to the ground state (G). In addition, the self-trapped exciton barrier (and the barrier E^* between the minimum of the self-trapped exciton potential curve and its intersection with the ground state potential curve are assigned).

from (E) to (G) are not observed, we assume that radiative transitions only occur from (STE). As a system of two coupled electron spins (electron and hole), the STE has a singlet state with fast lifetime τ_s and triplet states with long lifetime τ_t. Thereby the splitting energy Δ between singlet and triplet states can reach a few meV due to the strong confinement in the nanocrystals. The temperature dependence of the recombination times from these states was discussed earlier by Calcott *et al.*[8] for quantum confined exciton states in porous silicon. The same temperature dependence is now applied for the radiative STE recombination. This dependence is given by the equation:

$$\tau_r = \frac{3+\exp\left(-\frac{\Delta}{kT}\right)}{3\tau_t^{-1}+\tau_s^{-1}\cdot\exp\left(-\frac{\Delta}{kT}\right)}, \tag{2}$$

where the lower triplet state is assumed to have three times the degeneracy of the upper state.

A possible mechanism of a nonradiative recombination from (STE) states might be a tunneling process under barrier E^* into the ground state (G). The height of this barrier is an energy between the minimum of the (STE) state potential curve and its intersection with the ground state (G) potential curve (Fig. 5). The probability of this kind of recombination is proportional to the temperature ($\tau_{nr} \sim T^{-1}$).[9] Therefore the time of the STE recombination can be determined by the equation:

$$\tau^{-1}(T) = \tau_r^{-1}(T) + \tau_{nr}^{-1}(T), \tag{3}$$

where τ_r is the radiative recombination time and τ_{nr} is the nonradiative recombination time. Since the STE formation time, which can be estimated from the rising part of $I(t)$, is much faster than the decay of the integrated PL the observed decay time is mainly determined by the recombination of the (STE) state. As demonstrated in Fig. 2, Eq. (3) allows to fit the temperature dependence of the decay time using values of 90 μs (at $T=300$ K) for the nonradiative STE recombination time, 1.5 ms and 40 μs for the triplet and singlet (STE) lifetime, respectively, and 5.5 meV for their splitting energy. The fitting with these values of the decay times gives a dominant contribution to the decay time τ of the nonradiative decay time τ_{nr} at high temperatures (>60 K) and of the radiative decay time τ_r at lower temperatures (<60 K). It is necessary to note that even in the case of a temperature independent radiative recombination by setting $\Delta=0$ a good agreement with the observed temperature dependence of the decay time could be obtained, however, only a temperature dependent STE radiative recombination $\tau_r(T)$ can explain the temperature behavior of the parameter $\beta(T)$ and a spectral dependence of the decay time in the range between 10 and 60 K as shown in Fig. 4.

B. Temperature dependence

As discussed by Cullis *et al.*[10] the determination of a decay time from a nonexponential decay curve gives similar values by applying a ''stretch-exponential,'' a multiexponential fitting or when the decrease of the PL intensity by a factor of e is used. In the case of a ''stretch-exponential'' function, however, the fitting parameter $\beta(T)$ gives additional information about the dispersion of recombination times and can be analyzed together with the temperature dependence of the decay time. In addition, the temperature behavior of the parameter $\beta(T)$ gives a hint to the temperature dependent relation between radiative and nonradiative recombination from the (STE) states, which only give a contribution to the decay time. We assume that the dispersion factor $\beta(T)$ has different values for radiative β_r and nonradiative recombination β_{nr}. At higher temperatures the parameter $\beta(T)$ takes a constant value $\beta=0.73$, which is attributed to a dominating nonradiative STE recombination thus the value of $\beta(T)$ is defined by the value of β_{nr}. At lower temperatures ranging between 10 and 60 K there is a contribution of both recombination channels thus $\beta(T)$ which decreases with decreasing temperature is composed of both β_r and β_{nr}. From the value of $\beta(T)$ we conclude that the nonradiative recombination times show a lower dispersion than the radiative recombination times which can vary more due to crystal confinement and nonuniformity[11] and due to the dependence on the configuration coordinate.[5]

For an explanation of the temperature dependence of the PL intensity we have to consider the efficiency of each recombination channel. The formation of a STE is a temperature-activated process. So, at low temperatures, as we mentioned above, recombination via nonradiative centers from excited state (E) is a competitive process to radiative recombination via STE. In that case the probability to form (STE) state is:

$$C_{form}(T) = \frac{c_{STE}(T)}{c_{STE}(T)+c_{NS}}, \tag{4}$$

where $c_{STE}(T)=c_0\exp(-\vartheta/kT)$ is a probability to overcome the barrier ϑ defined in Fig. 5, c_{NS} is the probability to recombine nonradiative from (E) state. At higher temperatures ($kT>\vartheta$) a STE formation practically does not depend on temperature, but the temperature dependence of the PL intensity is determined by the radiative and nonradiative STE recombination:

$$C_r(T)=\frac{\tau_r^{-1}(T)}{\tau_r^{-1}(T)+\tau_{nr}^{-1}(T)}, \tag{5}$$

where τ_r and τ_{nr} are taken from Eq. (3). As mentioned above the probability of the STE nonradiative recombination $\tau_{nr}^{-1}(T)$ increases with temperature therefore the part of excitons which recombine radiatively decrease. A fitting of the PL temperature dependence given in Fig. 2 by the expression:

$$I_{PL}(T)\sim C_{form}(T)\cdot C_r(T) \tag{6}$$

gives a value of about 1.6 meV for the barrier ϑ. Additionally, the free parameters c_{NS} and c_0 in Eq. (4) have been chosen to set the PL efficiency lower than 1% over the entire temperature range.

C. Spectral dependence

At room temperature the decay time is primarily determined by the nonradiative recombination time from the STE state. The parameter $\gamma\approx 0.3$ eV, obtained from the spectral dependence of the decay time at 300 K, which is much larger than kT, supports the suggestion that a tunneling mechanism is involved in the STE nonradiative recombination process. The probability of the tunneling is a function of the barrier E^*, the height of which depends on the nanocrystal size. This leads to a dependence of the nonradiative recombination probability on the recombination energy also being a function of the nanocrystal size. An exponential behavior of the probability on the recombination energy can be obtained in the case of a tunneling through a square barrier with the condition that the height of the barrier is much greater than its change with nanocrystal size.[12] With the same assumption for any barrier shape one can expect a similar dependence which explains the observed behavior at 300 K in our samples.

At lower temperatures (<60 K) there is a contribution of a radiative recombination in the decay time which leads to a decreasing slope of the spectral dependence. These changes indicate some spectral dependence of the radiative decay time which is explained by a dependence of the splitting energy between singlet and triplet STE states on the nanocrystal size and thus on energy as shown in Fig. 6. The splitting energy $\Delta(E)$ was obtained by a fitting procedure considering the temperature dependence of the decay time at a certain emission energy $\tau^{-1}(E,\Delta(E),T)=\tau_r^{-1}(\Delta(E),T)+\tau_{nr}^{-1}(E,T)$ and using constant values for singlet τ_s and triplet τ_t recombination times, which were obtained before [see Eqs. (2) and (3)]. Furthermore, the previously obtained spectral dependence of the nonradiative recombination time $\tau_{nr}(E,T)\sim T^{-1}\cdot\exp(-E/\gamma)$ from the STE state was taken into account. Figure 6 shows that the splitting energy tends to decrease with decrease of the energy, which corresponds to an increasing nanocrystal size. Calcott *et al.*[8] reported the same dependence for porous silicon in the range 1.8–2.3 eV, while in our case the spectral dependence of the splitting energy Δ is observed in the range 1.4–1.7 eV. However, the obtained dependence is in agreement at 1.7–1.8 eV. In addition, Fig. 6 shows the relation $\Delta\sim(E-E_g)^{1.5}$ where $E_g=1.17$ eV is the 2 K band gap energy of bulk Si and the constant of proportionality is fixed by the calculation at $E=1.4$ eV. This relation, discussed in Ref. 8, was calculated in effective-mass theory for localized quantum-confined excitons. Experimental results give a lower steepness coefficient 1.4 and can be due to stronger STE localization. Probably, a calculation of singlet-triplet splitting for localized self-trapped exciton as a function of nanocrystal size should be performed.

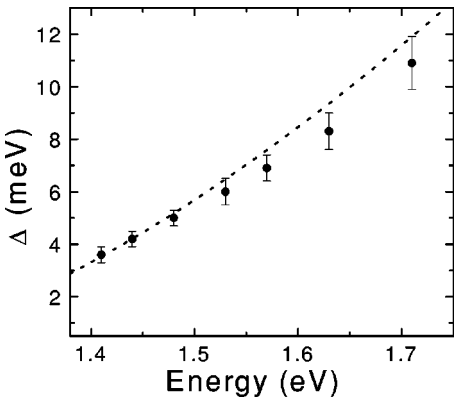

FIG. 6. Spectral dependence of the split energy between singlet and triplet (STE) states. (The dashed curve is the exchange splitting calculated in a simple effective mass theory with no adjustable parameters (Ref. 8).

V. CONCLUSIONS

In conclusion, the temperature and spectral dependence of the PL decay time together with the temperature dependence of the PL intensity from Si nanocrystals have been investigated. The obtained results have been explained using the model of a self-trapped exciton which is localized on a Si-Si bond at the nanocrystal surface and considering a nonradiative STE recombination due to tunnelling. The radiative and nonradiative recombination times and the splitting energy between the singlet and triplet states of the self-trapped exciton have been evaluated from the experimental data. In addition, we estimate the self-trapped exciton barrier height.

ACKNOWLEDGMENTS

The authors are grateful to Dr. W. Skorupa, Dr. G. A. Kachurin, and Dr. I. E. Tyschenko providing Si nanocrystals samples used in this study. The work was partially supported by Russian Foundation for Basic Research Grant No. RFBR 02-17963 and Graduiertenkolleg ''Thin films and noncrystalline materials'' of the Technische Universität Chemnitz.

*Recent address: Institut für Physik, TU Chemnitz, D-09107, Chemnitz, Germany.

[1] L.T. Canham, Appl. Phys. Lett. **57**, 1046 (1990).

[2] F. Koch, V. Petrova-Koch, T. Muschick, in *Light Emission from Silicon*, edited by J. C. Vial, L. T. Canham, W. Lang, J. Lum. **57** (Elsevier, North-Holland, 1993), p. 271.

[3] Y. Kanemitsu, Phys. Rev. B **49**, 16 845 (1994).

[4] K.S. Zhuravlev, A.M. Gilinsky, and A.Yu. Kobitsky, Appl. Phys. Lett. **73**, 2962 (1998).

[5] G. Allan, C. Delerue, and M. Lannoo, Phys. Rev. Lett. **76**, 2961 (1996).

[6] G.A. Kachurin, K.S. Zhuravlev, and N.A. Pazdnikov *et al.*, Nucl. Instrum. Methods Phys. Res. B **127/128**, 583 (1997).

[7] A.J. Kenyon, P.F. Trwoga, C.W. Pitt, and G. Rehm, Appl. Phys. Lett. **73**, 523 (1998).

[8] P.D.J. Calcott, K.J. Nash, and L.T. Canham *et al.*, J. Phys.: Condens. Matter **5**, L91 (1993).

[9] S.D. Ganichev, W. Prettl, and I.N. Yassievich, Phys. Solid State **39**, 1703 (1997).

[10] A.G. Cullis, L.T. Canham, and P.D.J. Calcott, J. Appl. Phys. **82**, 909 (1997).

[11] J.B. Khurgin, E.W. Forsythe, G.S. Tompa, and B.A. Khan, Appl. Phys. Lett. **69**, 1241 (1996).

[12] J.C. Vial, A. Bsiesy, and F. Gaspard *et al.*, Phys. Rev. B **45**, 14 171 (1992).